

# A Numerical Study on Geotextile-Reinforced Slopes

Hardik V. Gajjar<sup>1</sup> and Veerabhadra M. Rotte<sup>1</sup>

<sup>1</sup>Civil Engineering Department, Institute of Infrastructure Technology Research and Management, Ahmedabad – 380026, India

[vmrotte@iitram.ac.in](mailto:vmrotte@iitram.ac.in)

**Abstract:** In recent times, use of geosynthetics has gained widespread acceptance and has been used as reinforcing component in numerous geotechnical engineering structures. During construction of geotextile reinforced slope, it become essential to maintain certain value of factor of safety for each stages of construction. In this paper, a numerical study on slopes reinforced with and without geotextiles is presented. To capture the trend of development of axial forces in the geotextile layers under plastic analysis, four different slope inclinations ( $\beta$ ) (i.e.  $\beta= 45^\circ, 60^\circ, 75^\circ$  &  $90^\circ$ ) with slope height of 7 m were selected. Reinforced slopes were provided with equal number of geotextile layers along with uniform length ( $L_g$ ) of 6.4 m. The uniform vertical spacing ( $S_v$ ) of 1.0 m between any two geotextile layers was chosen. To simulate staged construction method which is adopted at site, finite element tool PLAXIS 2D was used for stability analysis. The construction of slopes was simulated in 7 stages of equal height for all the slope inclinations. The results showed that minimum axial forces were developed at the top most geotextile layer for all the four slope inclinations ( $\beta= 45^\circ, 60^\circ, 75^\circ$  &  $90^\circ$ ). Maximum axial forces were observed to develop in all geotextile layers for the slope having  $\beta = 90^\circ$  when it compared to other slope inclinations. With an increase in axial stiffness (EA) of geotextile layers by 100 %, it was noticed that only 16 % increase in axial force at the bottommost geotextile layer for the slope with  $75^\circ$  inclination.

**Keywords:** Axial Force, Slope Inclinations, Reinforcement Stiffness, Geotextile Reinforced Slopes

## 1 Introduction

Geotextile reinforced slopes (GRS) are mainly compacted embankments which are incorporated with geotextile layers as a reinforcement element. In geotextile-reinforced slopes, firstly failure plane is assumed and the length of geotextile beyond the failure plane is considered for resisting moment. Resisting moment depends upon the tensile capacity, interface friction developed between geotextile and soil and placing pattern of reinforcements. Koerner (1990) provided analysis method of geotextile-reinforced slopes for  $c-\phi$  soil using limit equilibrium concept. Mandal and Labhane (1991) carried out studies on geotextile-reinforced slopes. Lengths of geotextile in the top and bottom portion of the slope were varied for various slope

inclinations and soil properties. It was noticed that for steeper slope the length of geotextile for top layer was kept higher as compared to bottom layer to enhance the stability of slope. Jewell (1991) provided the design charts for overall stability as well as local stability of georeinforced slope. Holtz et al. (1998) provided design guideline and construction guideline for geosynthetic slope on soft soil strata. Duncan (1996) presented the advantages of finite element analysis over conventional limit equilibrium design. Griffiths and Lane (1999) took various cases to explain and validate finite element methods. Bergado et al. (2002) conducted stability analysis of embankment with and without reinforcement using PLAXIS 2D and concluded that single layer of high-strength geotextile (HSG) increases the critical slope height up to 1.5 times higher than that of the unreinforced case. HSG can significantly reduce vertical as well as horizontal displacement during plastic analysis. Zornberg and Arriaga (2003) conducted digital image analysis and centrifugal testing to understand the strain distribution in geotextile reinforced slope. The centrifuge model results show that maximum tensile strain was observed at mid height of the slope rather than at the bottom of the slope. Viswanadham and Konig (2008) used digital analysis technique to see the displacement of the markers glued in the reinforcement layers. This displacement of markers was used to analyze the strain distribution within the layers under various settlements stages. Analyses show that peak strain was observed just below the crest of the slope. Sommers and Vishwanadhan (2009) conducted centrifuge testing to see the influence of vertical spacing of reinforcement layers on stability of the slopes. They concluded that placing geotextile layers closely at mid height of the slope can turn out to be effective when footing is near to the crest of the slope. Tiwari and Samadhiya (2016) delineated the peak tension force in geotextile layers under various stiffness values.

## **2 Problem Description**

Available literature shows diverse opinions regarding the development of maximum axial force along slope height. Few literatures show that researchers have assumed maximum axial force at the toe of the slope. Other researchers found maximum axial force at mid height of the slope. In the present work, a parametric study has been carried out on geotextile reinforced slope using finite element based software PLAXIS 2D to identify the location of maximum axial force along geotextile layers for various slope inclinations ( $\beta$ ).

## **3 Modeling GRS in PLAXIS 2D**

The finite element method (FEM) has become essential tool in modeling and simulation of advanced engineering projects. In building complex engineering projects, engineer and designer go through a complicated process of modeling, simulation, visualization, analysis, design, prototyping and testing. In all this phases FEM become a standard tool. The behavior of physical phenomenon in a system depends upon the geometry, property of the material or medium, boundary conditions, initial and final loading conditions. In nature, most of the problem exists in

sophisticated geometry and difficult boundary conditions. Creating the geometry model is the first step toward preparation of finite element model. Geometry is nothing but the representation of problem statement. Geometry is prepared using points and lines. Once the required geometry is prepared, multiple soil strata can be assigned in it along with structural objects. Once the geometry is made, it is discretized into smaller pieces known as elements or cells, this process is usually referred as meshing. As the numbers of elements increase it increases the computational time of the simulation. Meshes should be selected according to the nature of the problem. For two-dimensional problems, the finite elements are usually triangular (3 nodes) or quadrilateral shape. If there are curved boundaries or curved material interfaces, the higher-order elements, with mid-side nodes should be used. In many cases, geometric discontinuities suggest a natural form of subdivision. In two-dimensional plane strain situations, the displacement field is characterized by the two global displacements  $u$  and  $v$ , in the  $x$  and  $y$  coordinate directions respectively. In the displacement-based finite element method, the primary unknown quantity is the displacement field which varies over the problem domain. Stresses and strains are treated as secondary quantities which can be found from the displacement field once it has been determined.

$$[K_E]\{d_e\} = \{R_E\} \quad (1)$$

$$\{d\} = \begin{Bmatrix} u \\ v \end{Bmatrix} = [N] \begin{Bmatrix} u \\ v \end{Bmatrix}_n = [N]\{d\}_n \quad (2)$$

$$\epsilon_x = \frac{\partial(u)}{\partial x} \quad (3)$$

$$\epsilon_y = \frac{\partial(v)}{\partial y} \quad (4)$$

Where  $[K_E]$  is the element stiffness matrix,  $\{d_E\}$  is the vector of incremental element nodal displacements and  $\{R_E\}$  is the vector of incremental element nodal forces. In an equation 3 and 4  $\Delta\epsilon_x$  and  $\Delta\epsilon_y$  are the strain corresponding to the displacements. In an equation 2 'N' is the shape function. In PLAXIS 2D the analysis is done in three stages: (i) Gravity loading: stress due to gravity is calculated (ii) Plastic Analysis: show the actual deformation of slope (iii) Safety analysis. In design of an embankment, it is necessary to check the stability during each stage of construction along with overall stability. Phi-c reduction method (Shear strength reduction) has been used in current studies for reinforced slopes. Several earlier research works show successful usage of this method (Griffith and Lane 1999). Phi-c reduction calculation type was used, which reduces the values of cohesion ( $c$ ) & angle of internal friction ( $\phi$ ) in steps until the soil body fails, the following equation is used

$$\frac{C}{C_r} = \frac{\tan \phi}{\tan \phi_r} = \sum M_{sf} \quad (5)$$

$c_r$  and  $\phi_r$  are the reduced strength parameter that are just large enough to maintain equilibrium. The safety factor is then defined as the value of  $\sum Msf$  at the failure, provided that at failure a more or less constant value is obtained for number of successive load steps. For most safety analyses  $\sum Msf = 0.1$  is an adequate first step to start up the process. During the calculation process, the development of the total multiplier for the strength reduction  $\sum Msf$  is automatically controlled by load advancement procedure.

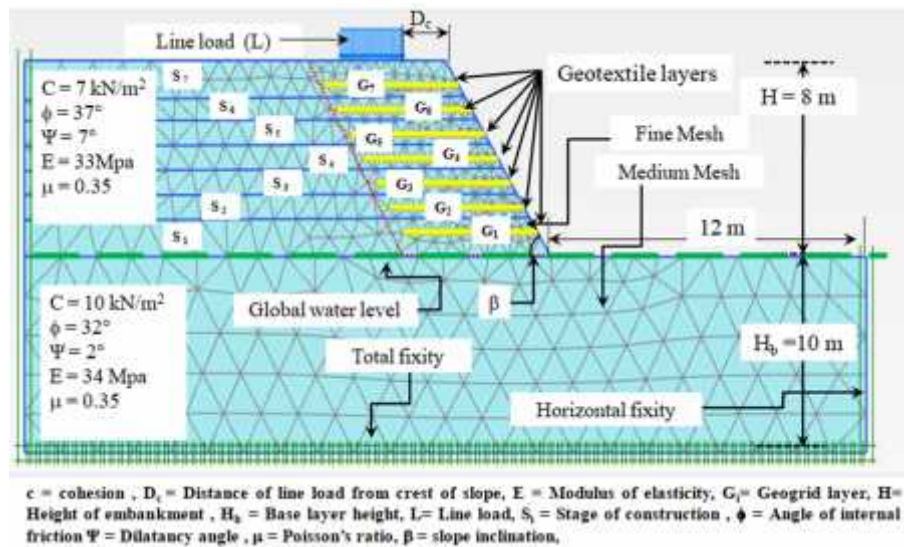


Fig. 1. Modeled Geotextile reinforced slope adopted for finite element analysis

Table 1. Summary of the soil properties and reinforcement parameters used in FEA

Soil/ Reinforcement	$\phi$ ( $^{\circ}$ )	$c$ ( $\text{kN/m}^2$ )	$\phi$ ( $^{\circ}$ )	$\mu$	$E$ (MPa)	$EA$ ( $\text{kN/m}^2$ )	$L_g$ (m)	$S_v$ (m)
Embankment	37	7	37	0.35	33			
Base Layer	32	10	32	0.35	34		N.A	
Geotextile			N.A			4500-13500	6.4	1.0

$c$  = cohesion,  $E$  = Modulus of Elasticity,  $EA$  = Reinforcement Stiffness,  $L_g$  = Length of Geotextile, N.A = Not Applicable,  $S_v$  = Vertical Spacing of Geotextile Layers,  $\phi$  = Angle of Internal Friction,  $\Psi$  = Dilatancy Angle,  $\mu$  = Poisson's Ratio

## 4 Model Validations

Model validation was carried out in two phase i.e. (i) validating values of factor of safety for different values of  $c_e/c_f$  ( $c_e$  = cohesion for foundation soil and  $c_f$  = cohesion of embankment) (ii) validation of factor of safety under reinforced condition. To validate the methodology adopted for the analysis of unreinforced slope under various shear strength value, embankment having weak foundation layer has been taken from the literature (Example 4 Griffith and Lane 1999). Here,  $c_e/\gamma H = 0.25$  was kept constant in all the cases generated to validate the model. Figure 3 shows the geometry adopted for the model validation. The slope inclination was kept as  $26.56^\circ$ . The height of the embankment (H) was kept same as the height of foundation layer as mentioned in the literature. The shear strength of the homogenous embankment was kept constant, while shear strength of the foundation layer was varied. The validation model shows a good agreement with the literature for all the values of  $c_e/c_f$ , the results obtained from the analysis were compared in the form of factor of safety. Figure 2 shows the validation of computed factor of safety under various values of  $c_e/c_f$ . To validate the methodology adopted for the analysis of geotextile reinforced slope, slope having inclination of  $45^\circ$  and four geotextile layer of equal length were adopted (Han et al., 2002). Moreover the vertical spacing was kept constant for any two geotextile layer. Tensile stiffness of the geotextile was kept as 1000 kN/m. Geometry for the validation of geotextile reinforced slope is shown in Figure 4. Soil properties used in the validation work are summarized in Table 2. The factor of safety (FOS) value obtained was 1.51 through strength reduction method for reinforced conditions. Corresponding FOS for reinforced slope obtained by finite difference program, FLAC was 1.55 reported by Han et al, 2002.

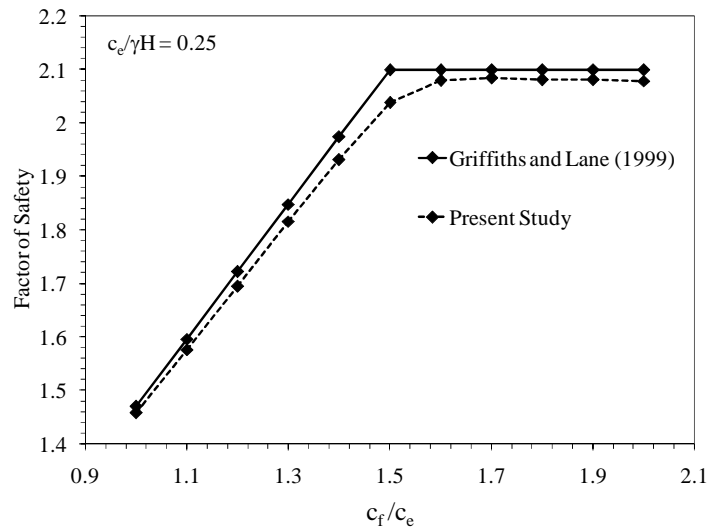
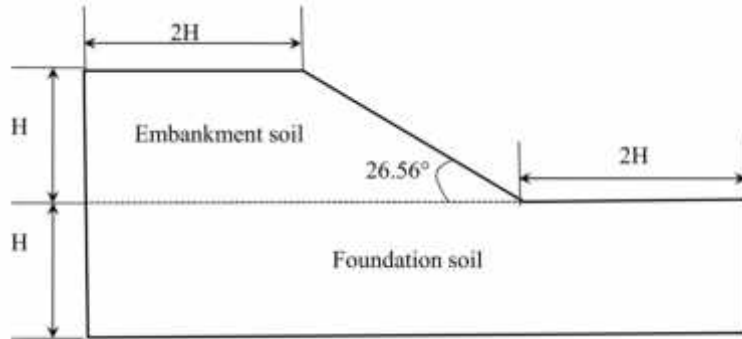
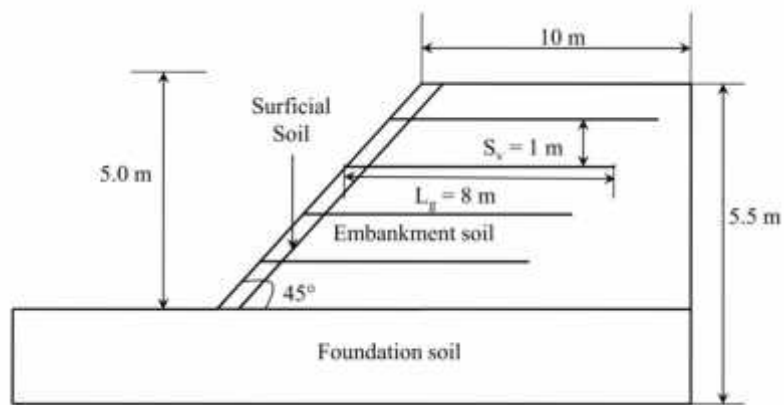


Fig. 2. Validation of computed factor of safety under various values of  $c_e/c_f$



**Fig. 3.** Geometry for the validation of FOS of slope under unreinforced slope (Griffith & Lane 1999)



**Fig. 4.** Geometry for the validation of FOS of slope under unreinforced slope (Han et al., 2002)

**Table 2.** Summary of soil properties used for validation of reinforced slope

Soil	$\gamma$ (kN/m <sup>2</sup> )	c (kPa)	$\phi$ (°)	$\mu$	E (MPa)
Embankment	18	2	30	0.3	20
Foundation	18	100	24	0.3	1000
Surficial	18	20	30	0.3	20

c = Cohesion, E = Modulus of Elasticity,  $\phi$ = Angle of Internal Friction,  $\gamma$  = Unit Weight,  $\mu$  = Poisson's ration of soil

## 5 Results and Discussions

### 5.1 Effect of Slope Inclination

To capture the trend of development of axial force in the geotextile layers under plastic analysis various slope inclination were modeled having same number of geotextile layers and length of each geotextile were kept same. Required length for the geotextile layer under selected soil inclinations and soil parameters were selected as per Jewell's charts. The selected length for all the geotextile layer was 6.4 meter. The uniform vertical spacing of 1.0 m between any two geotextile layers was chosen. Sequential construction method was adopted during analysis process in which whole soil strata was divided into 7 stages. During analysis of stage 1 only bottom most geotextile layer i.e. G1 was kept active, while for stage 2 bottom two layers were kept active (i.e. G1 and G2). Likewise similar fashion was adopted for remaining all stages. The trend capture for development of axial force for the slope inclination ( $\beta$ )  $\geq 45^\circ$  was almost same. As the slope inclination increase, the maximum horizontal displacement was observed on the upper most portions of the slopes rather than at toe of the slope. While for  $\beta \leq 45^\circ$  maximum horizontal displacement was observed at bottom as well as middle portion of slope. Figure 6, 7 and 8 shows the development of the axial force along the stage construction for  $\beta = 75^\circ$ ,  $\beta = 60^\circ$  and  $\beta = 45^\circ$  respectively. For any project it is essential to check factor of safety at each stage. Figure 9 shows the reduction in factor of safety along with stage construction for various slope inclinations. For slope inclination of  $75^\circ$  the variation in the safety factor is least compare to other slope inclination. The intensity of horizontal displacement was higher compare to vertical displacement irrespective to slope inclination.

Contradicting current design assumptions, the distribution of axial force with height does not show a triangular pattern with a maximum value at the toe. Instead, the results show that during plastic analysis for  $\beta < 45^\circ$  maximum axial force is located approximately at mid-height of the slope. With increase in the slope inclination the location of the maximum axial force is shifting towards the bottom reinforcement layers. With the slope inclination  $> 60^\circ$  or  $65^\circ$ , location of maximum overburden shifts downwards at the toe of the slope. The magnitude of maximum axial force almost increases to 7 times when the slope inclination is increase from  $45^\circ$  to  $75^\circ$ .

### 5.2 Effect of Reinforcement Stiffness

To decide the initial value of stiffness (EA) trial and error method was adopted. The minimum value at which slope with  $\beta = 90^\circ$  remains stable was selected. For  $\beta = 90^\circ$  with increase in stiffness by 100% from the initial value percentage increase in axial force in bottom most layer of geotextile (i.e. G1) was nearly 14.63%. Moreover with increase in stiffness value by 200% from the initial value, the percentage increase in axial force was observed to be 19.51 % which is also reflected inthe Figure 5.

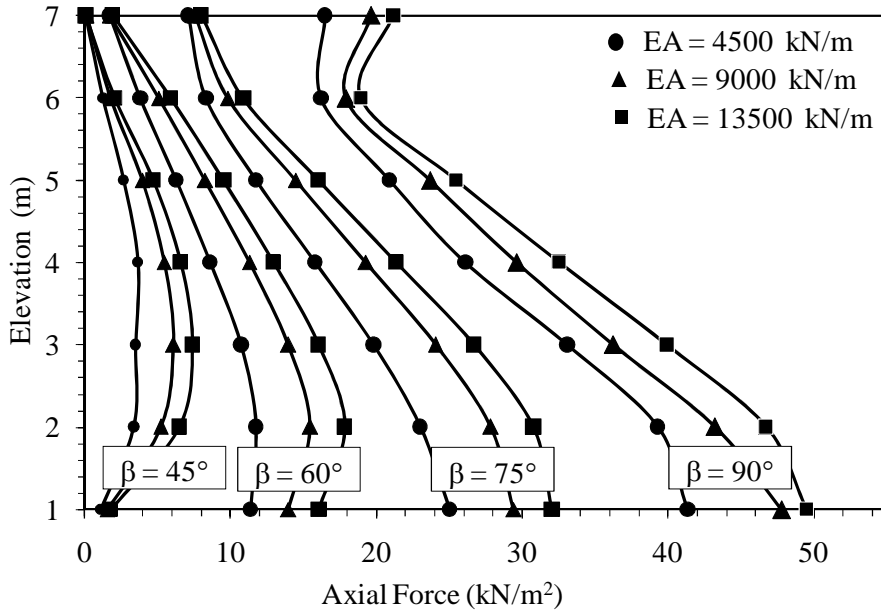


Fig. 5. Influence of reinforcement stiffness on development of axial force

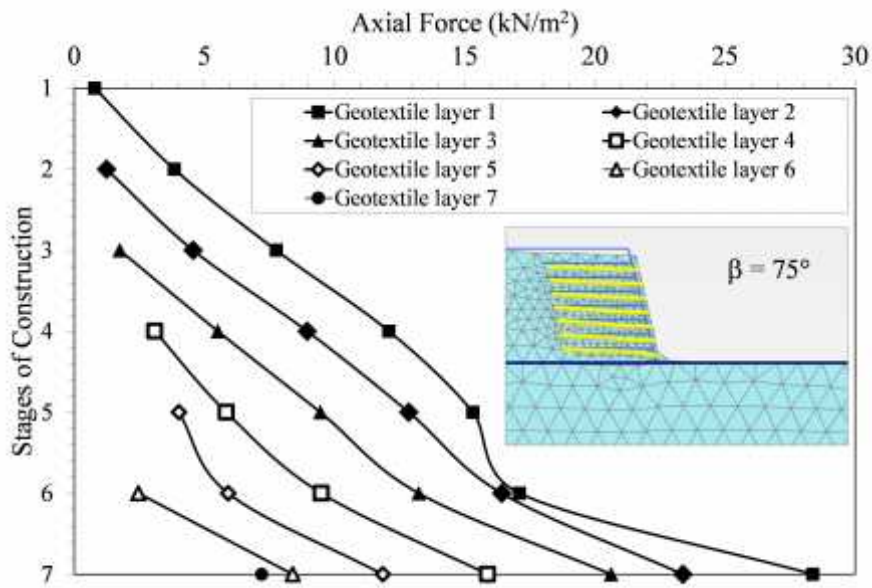


Fig. 6. Development of axial force for geotextile layers for various stages of construction with  $\beta = 75^\circ$

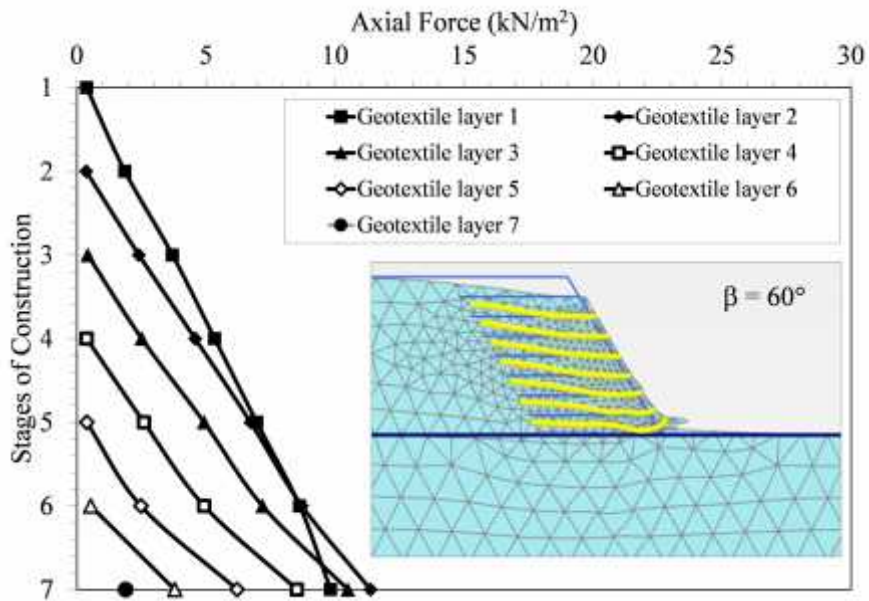


Fig. 7. Development of axial force for geotextile layers for various stages of construction with  $\beta = 60^\circ$

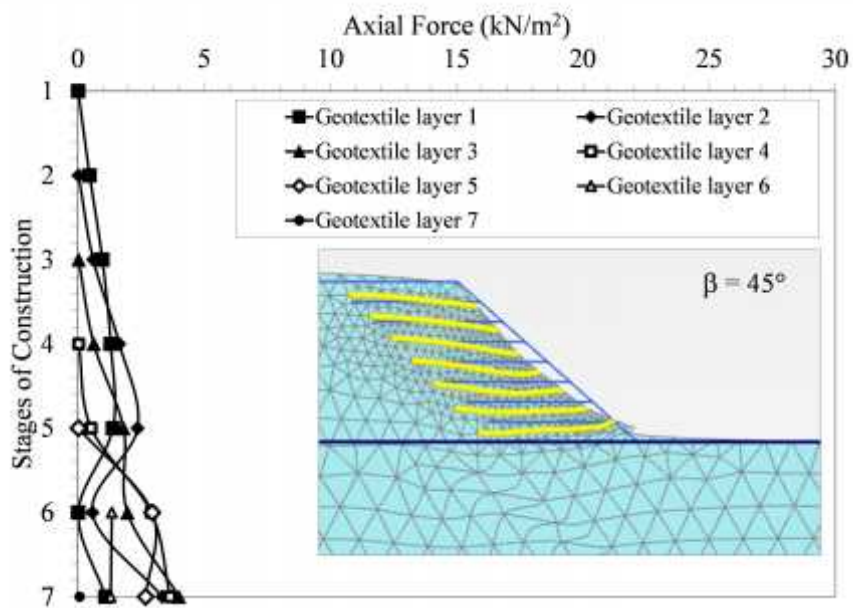


Fig. 8. Development of axial force for geotextile layers for various stages of construction with  $\beta = 45^\circ$

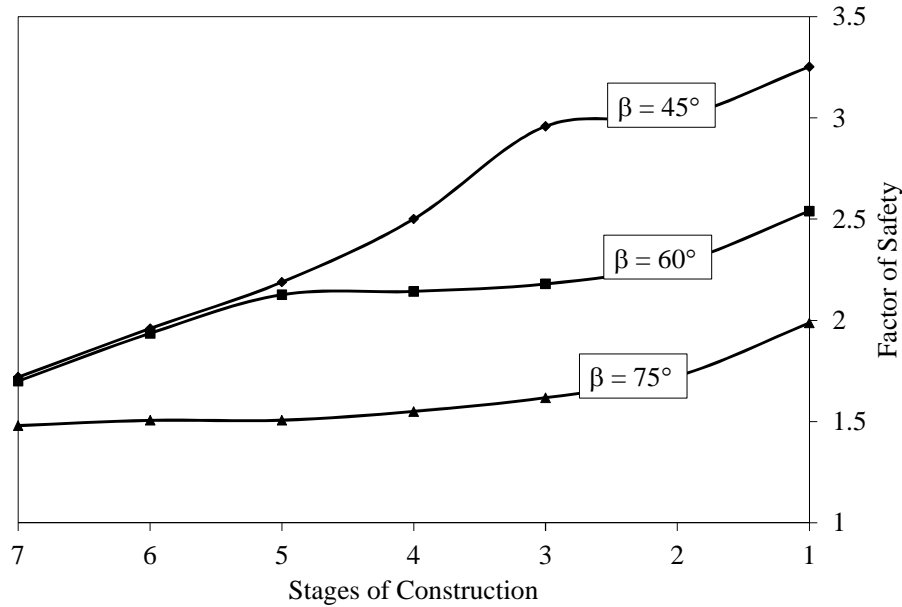


Fig. 9. Variations in factor of safety during stage construction

## 6 Conclusions

A Numerical parametric analysis has been performed in order to understand the axial force distribution across geotextile layers for various slope elevations. The following conclusions can be drawn from this study.

- Development of maximum axial force in the reinforcement layers gets influence by slope inclinations. The location of maximum axial force tends to shifts downward with increase in slope inclinations.
- Stresses developed in bottom most geotextile layer in all steep slopes increases with increase in stages of construction. Hence due to this axial force tends to be increasing. For slope having lower inclination angle maximum axial force is obtained at 2<sup>nd</sup> or 3<sup>rd</sup> stage of construction.
- Location of maximum axial force is not influenced by the stiffness of the geotextile layers.
- Maximum axial forces were observed to develop in all geotextile layers for the slope having  $\beta = 90^\circ$  when it compared to other slope inclinations. With an increase in axial stiffness (EA) of geotextile layers by 100 %, it was noticed that only 16 % increase in axial force at the bottommost geotextile layer for the slope with 75° inclination.

## References

1. Bergado, D.T., Long, P.V., Murthy, B.R.S.: A case study of geotextile reinforced embankment on soft ground. *Geotextile and Geomembrane* 20: 343-365 (2002).
2. BS 8006-1: Code of practice for strengthened /reinforced soil and other fills (2006).
3. Duncan, J.M.: State of the Art: Limit equilibrium and finite element analysis of slopes. *Journal of Geotechnical Engineering, ASCE* 122 (7): 577-596 (1996).
4. Griffith, D. V., Lane, P.: Slope stability analysis by finite elements. *Geotechnique* 49 (3): 387-403 (1999).
5. Han, J., Leshchinsky, D., Shao, Y.: Influence of tensile stiffness of geosynthetic reinforcement on performance of reinforced slopes, *Proceedings in Geosynthetics-7 ICG-Delmas* 197-200 (2002).
6. Holtz, R.D., Barry, R.C., Berg, R.R.: *Geosynthetic design and construction guidelines*. (1998)
7. Jewell, R.A., Paine, N., Wood, R.I.: Design methods for steep reinforced embankments. *Proceedings of the Polymer Grid Reinforcement Conference London* 70-81 (1984).
8. Koerner R.M.: *Designing with geosynthetics*, 5<sup>th</sup> edition, Pearson Prentice Hall, New Jersey (2005).
9. Mandal, J. N., Labhane, L.: A procedure for the design and analysis of geosynthetics reinforced soil slope." *Geotechnical and Geological Engineering* 10: 291-319 (1992).
10. Sommers, A.N, Vishwanadham B.V.S.: Centrifugal model test on the behavior of strip footing on geotextile reinforced slopes. *Geotextile and Geomembranes* 27: 497-505 (2009).
11. Vishwanadham B.V.S., König, D.: Centrifuge modeling of geotextile reinforced slopes subjected to differential settlement. *Geotextile and Geomembranes* 27: 77-88 (2009).
12. Zornberg, J.G., Arriaga, F.: Strain distribution within geosynthetic reinforced slope. *Journal of Geotechnical and Geoenvironmental Engineering* 123 (1): 32-45 (2003).